Heat Transfer in Rotating Rectangular Cooling Channels (AR=4) With Angled Ribs

Todd S. Griffith
e-mail: ddot1976@yahoo.com
Research Assistant

Luai Al-Hadhrami
Research Assistant

Je-Chin Han
M.C. Easterling Endowed Chair

Turbine Heat Transfer Laboratory,
Department of Mechanical Engineering,
Texas A&M University,
College Station, TX 77843-3123

An investigation into determining the effect of rotation on heat transfer in a rib-roughened rectangular channel with aspect ratio of 4:1 is detailed in this paper. A broad range of flow parameters have been selected including Reynolds number (Re=5000–40000), rotation number (Ro=0.04–0.3) and coolant to wall density ratio at the inlet $(\Delta\rho/\rho)_i = 0.122$. *The rib turbulators, attached to the leading and trailing surface, are oriented at an angle* ($\alpha = 45$ deg) *to the direction of flow. The effect of channel orientations of* $\beta = 90$ *deg and 135 deg with respect to the plane of rotation is also investigated. Results show that the narrow rectangular passage exhibits a much higher heat transfer enhancement for the ribbed surface than the square and 2:1 duct previously investigated. Also, duct orientation significantly affects the leading and side surfaces, yet does not have much affect on the trailing surfaces for both smooth and ribbed surfaces. Furthermore, spanwise heat transfer distributions exist across the leading and trailing surfaces and are accentuated by the use of angled ribs. The smooth and ribbed case trailing surfaces and smooth case side surfaces exhibited a strong dependence on rotation number.*
[DOI: 10.1115/1.1471525]

Keywords: Enhancement, Heat transfer, Rotating, Roughness, Turbines

Introduction

As the world becomes exceedingly industrialized, there develops an ever-increasing demand for energy. Extensive research efforts have recently focused on methods for reducing the consumption of energy. One area focused on improvements in efficiency is the turbomachinery industry. There is a constant drive to decrease the cost associated with repairing a gas turbine as well as increasing the fuel efficiency. With the wide spread application of turbines from power generation to aircraft propulsion, the cost saving can be enormous. One method of increasing the efficiency of a turbine as well as the thrust of an aero-turbine is by increasing the combustion temperature. This poses a major problem in the hastened degradation of temperature sensitive components of the turbine, principally the turbine blades. To counter the high turbine inlet temperatures (1600–1800 K), the physics of turbulent heat transfer are investigated in a cooling model. Turbine blades incorporate internal cooling passages to extract the thermal energy absorbed from the hot combustion gases. This prolongs the life of the blade as well as allowing for increased combustion temperatures, which ultimately increases performance of the turbine.

A small amount of pressurized air is extracted from the compressor and injected into the turbine blades via the cooling air bypass. This relatively low enthalpy gas is forced through the internal cooling passages of the turbine blades, convectively extracting heat from the internal walls. For further thermal protection of the blade, a portion of the internal cooling air is ejected through tiny holes in the walls and tip of the blade, creating a cool film thermal boundary.

When considering the effects of rotation, certain flow phenomena are exhibited that are not observable in the stationary reference frame. Forces are generated under a rotational reference frame, principally the Coriolis and buoyancy forces. These forces generate secondary flows in the plane orthogonal to the mean flow direction. For radial outward flow, the Coriolis and buoyancy forces combine to shift the velocity profile toward the trailing surface. The coolant flow migrates along with the heat transfer augmentation toward the trailing surface. This rotationally induced migration of the cooler core flow results in the advantageous enhancement of heat transfer at the trailing surface, but it is typically balanced by the disadvantageous reduction in heat transfer from the leading surface. As with most temperature sensitive components, thermal failure in an isolated region is oftentimes just as problematic as failure of the entire component. This is why it is important to analyze the heat transfer phenomenon segment by segment along the length of the blade.

The aspect ratio of the channel also has a profound impact on the effect of rotation. Moving from the mid-chord to the trailing edge of the blade, the channels must become more rectangular as the blade becomes thinner. The orientation of a 4:1 aspect ratio cooling channel in a gas turbine blade is shown in Fig. 1. This thinning of the channel changes the effective secondary flow pattern from that of a square duct. For this reason, one cannot simply apply the knowledge of the rotationally induced flow patterns in a square channel to that of a rectangular channel. Therefore, an investigation of the rectangular channel is necessary to further understand the heat transfer characteristics of the internal cooling channels in a gas turbine blade.

To promote heat transfer in the internal cooling passage, various types of turbulators are used to trip the boundary layer. The onset of turbulence results in higher heat transfer by promoting mixing of the cooler core jet gases with the hot boundary layer at the walls. The most common and effective type of turbulator is referred to as the ''rib'' or ''trip-strip.'' These ribs appear as small rectangular surface protrusions, and are typically oriented at 45 deg to the direction of flow on the internal leading and trailing surfaces of the blade. When combining the effects of tripping the boundary layer (ribbed-turbulator) and rotational forces (Coriolis and buoyancy), entirely different turbulence and flow phenomenan are achieved. Combining into this equation the various shapes and sizes of internal cooling channels, it is clear that there is no one single solution that can be applied universally in the field of turbine heat transfer. For this reason, an experimental investigation into each combination of the previously mentioned parameters is necessary. Until now, published literature concerning the rotational effect on the regionally averaged heat transfer characteristics has not existed for the 4:1 aspect ratio duct.

Contributed by the Heat Transfer Division for publication in the JOURNAL OF HEAT TRANSFER. Manuscript received by the Heat Transfer Division August 14, 2001; revision received February 14, 2002. Associate Editor; H. S. Lee.

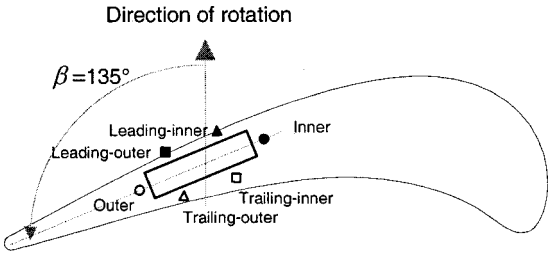

Fig. 1 Sketch illustrating orientation of a 4:1 aspect ratio channel in a gas turbine blade

There are numerous past studies on turbulent flow and heat transfer in the cooling channels of a gas turbine blade. Han and Park [1] published experimental investigations of the heat transfer phenomenon in a stationary rib roughened rectangular channel. Han et al. [2] performed a study of the effect of the rib angle on heat transfer distributions and pressure drop in a stationary square channel with two opposite in-line ribbed walls. These studies showed that the 60 deg and 45 deg V-shaped rib performs better than the 60 deg and 45 deg parallel rib. It was also concluded that the V-shaped rib out-performs 60 deg and 45 deg crossed ribs as well as the 90 deg rib. Wagner et al. [3,4] conducted detailed experimental investigation to determine the effects of rotation, or more specifically the effects of Coriolis and buoyancy forces on the regionally averaged heat transfer distribution of a serpentine square channel with smooth walls. This study determined that in the first pass, the effect of rotation created a thinner boundary layer on the trailing surface and a thicker boundary layer on the leading surface.

Parsons et al. [5] and Johnson et al. [6] studied the effects of channel orientation and wall heating condition on the regionally averaged heat transfer coefficients in a rotating two-pass square channel with ribbed walls. Parsons et al. [5] discovered that the heat transfer enhancement for the constant wall heat flux boundary condition was more pronounced when the duct is twisted 45 deg to the plane of rotation when compared to a channel oriented orthogonal to the plane of rotation. Johnson et al. [6] determined that the model orientation with respect to the rotation plane greatly affected the heat transfer distribution.

Dutta and Han [7] investigated the regionally averaged heat transfer coefficients in a rotating two-pass square channel with three different model orientations. They found that the orientation of the channel with respect to the plane of rotation affected the heat transfer distribution. More specifically, they determined that orienting the channel at an angle with respect to the plane of rotation reduced the effect of rotation when compared to the orthogonal channel orientation.

Until recently, most of the experimental studies have explored only square ducts. However, it is quite common to find rectangular cooling passages, particularly toward the trailing edge of a gas turbine blade. Since the profile of a turbine blade is curved, the exclusive use of square channels is not practical. Past research focused mainly on the square channel; therefore, published data for a rectangular cooling channel is rare. Al-Qahtani et al. [8] published a numerical prediction of the flow behavior and heat transfer in a rib-roughened, rotating, two pass rectangular channel of aspect ratio 2:1. An interesting description of the flow physics associated with rib flow is included in their investigation. Taslim et al. [9,10] investigated the heat transfer distribution in square and rectangular rib-roughened channels under rotation. They applied the liquid crystal technique to study the effect of rotation on wall heat transfer. It was discovered that the effects of rotation were more apparent in rib-roughened channels with a larger channel aspect ratio and a lower rib blockage ratio. This investigation studied only the heat transfer distribution in an orthogonal rotating channel.

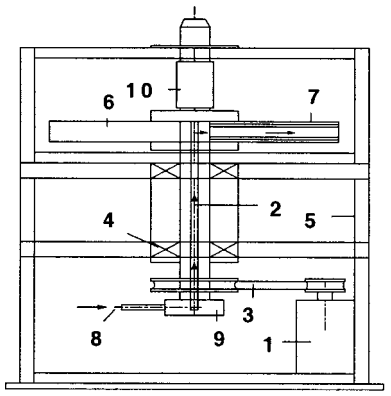

Fig. 2 Schematic of experimental rotating test rig

Willett and Bergles [11] performed a detailed investigation of the heat transfer in a narrow, 10:1 smooth rectangular channel oriented at 60 deg to the r-z plane. Most of their focus dealt with exploring the contribution of buoyancy forces under rotation. They found that the duct orientation induced a significant variation in the heat transfer coefficient in the spanwise direction. It was also found that the normalized Nusselt number at the far-aft-end of the trailing side (or the trailing-outer equivalent in this paper) is a strong function of rotation number and buoyancy number. However, they did not perform tests at an angle normal to the plane of rotation in order to determine how changing the duct orientation affects the heat transfer distribution within the rectangular channel, nor did they consider the effect of varying the surface configuration, such as the common ribbed surface. Also, most of their study presented data in streamwise averaged format, even though the data was taken at localized points. For a more comprehensive compilation of turbine heat transfer research, please see the book by Han et al. [12], the review paper by Han and Dutta [13], and the review paper by Dutta and Han [14].

Therefore, it is of interest to experimentally investigate the regionally averaged heat transfer distribution in a rotating, rectangular channel of aspect ratio 4:1. The fact that no such literature exists today on this subject raises the following questions:

1. How does the spanwise heat transfer distribution vary within a smooth and ribbed rectangular channel, and is it significant enough to require consideration when designing the cooling channels of a turbine blade?
2. Does the surface configuration and orientation of the rotating rectangular channel significantly affect the heat transfer distribution?
3. Do the narrow aspect ratio ducts exhibit different heat transfer distributions when compared to the square and rectangular channels of lower aspect ratio?

Answers to these questions are pursued in this paper.

Experimental Facility

The experimental test rig previously used by Dutta and Han [7] is utilized in this investigation (see Fig. 2). A variable frequency motor is connected via a gear-and-belt mesh to a hollow, rotating shaft. This shaft runs from the base of the test rig to the work platform and is attached orthogonal to the hollow, rotating arm. The test section is inserted inside the hollow rotating arm, which rotates in a plane orthogonal to the rotating shaft. A hand held optical tachometer is used to determine the rotational velocity of

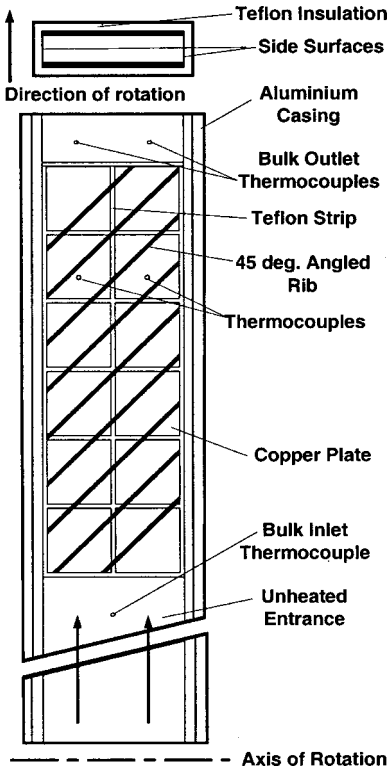

Fig. 3 Schematic of 4:1 test section

the arm. Thermocouple and heater wires are connected to a 100-channel slip-ring assembly mounted to the rotating shaft. The output of the thermocouples is transferred to a data logger. Fuse-protected power input to the heaters from the variac transformers is also transmitted through the slip ring assembly. Cooling air is pumped from a steady flow compressor, through an ASME orifice flow meter, then through the hollow rotating shaft, turning 90 deg and passing into the rotating arm, then through the test section and is finally expelled into the atmosphere.

The test section is a 0.5 in. by 2 in. by 6 in. long ($1.27\times5.08\times15.24$ cm) one-pass rectangular channel of aspect ratio 4:1 with a hydraulic diameter of $D=0.8$ in. The ratio of mean rotating radius to hydraulic diameter is $R/D=33$. The direction of airflow is radially outward from the axis of rotation. Two rows of copper plates are installed on both the leading and trailing surface to provide a grid for analysis of the spanwise variation in the regionally averaged heat transfer coefficient.

Figure 3 shows a detailed top view of the test section. The test section is divided into six cross-sections, each with six copper plates: two for the leading, two for the trailing, one for the outer and one for the inner surface. Moving along the direction of the flow (radially outward), there are six streamwise segments for a total of 36 copper plates in the entire test section. The channel length-to-hydraulic diameter ratio (L/D) is 7.5 with a ratio of 1.25 for each of the six cross-section segments. Each plate is separated by a 0.0626 in. (0.159 cm) thin strip of nylon to prevent heat conduction between plates. This is important since the objective is to study the spatial distribution of heat transfer.

The copper plates are mounted in a nylon substrate, which comprises the bulk of the test section. Pre-fabricated flexible heaters are installed beneath the leading and trailing surfaces, two to each surface. The outer and inner walls (or side walls) are each heated by a wire-wound resistance heater, which is also installed beneath the copper plates. All heaters supply steady, uniform heat flux to the copper plates. Sufficient power is supplied in order to maintain a maximum wall temperature of nearly 340 K for the corresponding section. This corresponds to an inlet coolant-to-wall density (temperature) ratio $(\Delta\rho/\rho)_i$ of 0.122 for every test. Thermal conducting paste is applied between the heater and copper plates to promote heat transfer from the heater to the plate. Each 1/8 in. (0.318 cm) thick plate has a 1/16 in. (0.159 cm) deep blind hole drilled in the backside in which a copper-constantan thermocouple is installed 1/16 in. (0.159 cm) from the plate surface with thermal conducting glue.

Two different surface configurations (smooth and 45 deg ribs) are studied as well as two different channel orientations with respect to the direction of rotation ($\beta=90$ deg and 135 deg). Figure 3 shows the ribbed surface configuration. The channel is rib-roughened on two opposite walls with 45 deg in-line ribs. The parallel rib configuration was chosen due to the widespread use of 45 deg parallel ribs in turbine blade cooling channels. The ribs are made of brass and are glued to the leading and trailing surfaces of the channel, resulting in a rib height-to-hydraulic diameter ratio (e/D) of 0.078 and a pitch-to-rib height (P/e) ratio of 10. The rib flow-attack angle, defined as the angle between the mean flow direction and the rib angle orientation (α), is maintained at 45 deg. The experiments were conducted for Reynolds numbers of 5000, 10,000, 20,000 and 40,000. The test section rotates at a speed of 550 rpm, resulting in a range of rotation number (Ro) from approximately 0.04–0.3.

Data Reduction

This investigation focuses on detailing the regionally averaged heat transfer coefficient at various locations within the internal cooling channel. This heat transfer coefficient is determined by the net heat flux from the heated plate to the cooling air, the surface area of the plate (A_p), the regionally averaged temperature of the plate, and the local bulk mean air temperature by the following:

$$h=q''_{\text{net}}/(T_w-T_{b,x}) \tag{1}$$

The net heat flux is calculated using the measured voltage and current supplied to the heater multiplied by the area fraction exposed to the respective plate minus the previously determined amount of heat losses due to external conduction, convection, and radiation energy escaping from the test section. This heat loss calibration is performed for both stationary and rotation experiments with a piece of insulation inserted inside the test section to inhibit natural convection. For this calibration, by knowing the amount of power supplied to the heater and measuring the temperature of the plate, it is possible to determine how much the heat is being lost into the environment using the conservation of energy principle. Equation (1) is used throughout the experiment, neglecting the change of area effect with the addition of ribs. That is, the heat transfer coefficient is calculated based on the projected area, neglecting the 28 percent increase in area due to the addition of ribs.

The regionally averaged wall temperature (T_w) is measured directly by the thermocouple installed in the blind hole on the back of each plate. The local bulk mean air temperature ($T_{b,x}$) is determined by a linear interpolation between the measured bulk air inlet and the average of two outlet temperatures (each installed at the midpoint of the two spanwise sections) due to the applicable constant heat flux assumption. Another method used to check the interpolation values is by performing an energy balance. It is reassuring to note that performing an energy balance to calculate the expected outlet temperature resulted in a close match to that of the average measured exit temperature value, typically to within 5 percent. Therefore the linear interpolation method is validated and is the method used in the calculation of the results presented in this paper. The energy balance equation is:

$$T_{b,i}=T_{\text{in}}+\sum_i (q-q_{\text{loss}})/\dot{m}c_p, \quad i=1,2\ldots6 \tag{2}$$

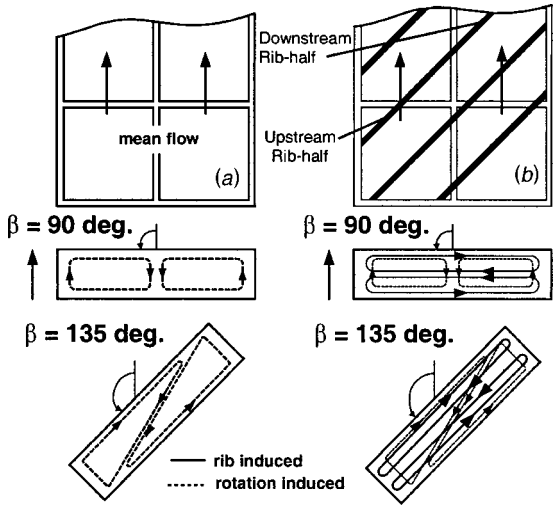

Fig. 4 Outward flow rectangular test section with: (*a*) smooth walls; and (*b*) 45 deg parallel ribs on leading and trailing surfaces.

To provide a common reference for each analysis, a correlation is used comparing the Nusselt number for the specific duct case to that of fully developed flow through a smooth stationary circular pipe at the same Reynolds number. For this investigation, the Dittus-Boelter correlation for heating ($T_w > T_{bx}$) is used:

$$\frac{\mathrm{Nu}}{\mathrm{Nu}_o} = \frac{hD}{k_{\mathrm{air}}} \frac{1}{(0.023\,\mathrm{Re}^{0.8}\mathrm{Pr}^{0.4})} \tag{3}$$

All air properties are taken based on the mean bulk air temperature with a Prandtl number (Pr) for air as 0.71.

Overall uncertainty for the regionally averaged heat transfer is predominantly dependent upon the difference between the wall temperature and the bulk air temperature, the net heat flux input and the ability to maintain a steady mass flow rate. As with most experiments, the uncertainty for this investigation decreases with the increasing magnitude of input parameters. For higher Reynolds numbers, the uncertainty has been determined to be nearly 7 percent. However, for lower Reynolds numbers (Re=5000), the uncertainty could be as much as 20 percent. The uncertainty analysis was performed using the Kline and McClintock [15] uncertainty analysis procedure.

Results And Discussion

Before any discussion of the physics associated with the thin rectangular duct proceeds, it is important to set up a labeling scheme for the various surfaces in the duct. This labeling scheme, seen in Fig. 1, will be used throughout this paper. The inner and outer surface side walls are named according to their location in the turbine blade. That is, the inner surface is closer to the mid-chord position of the blade (a relatively internal position), and the outer surface is closer to the trailing edge of the blade, and thus is closer to an external surface of the blade. The leading and trailing surfaces of the blade follow the conventional definitions of these surfaces, however each surface is subdivided into two surfaces in order to investigate the span-wise distribution of heat transfer along the major surfaces (leading and trailing). Therefore we have a total of six surfaces: leading-outer, leading-inner, trailing-outer, trailing-inner, outer, and inner. Because of the many intrinsic differences between square and rectangular ducts, a brief discussion on the secondary flow patterns generated by rotation and the ribs in a thin rectangular duct follows.

Secondary Flow Behavior. Figure 4 shows a conceptualization of the secondary flow patterns of a smooth and ribbed rotating duct. The smooth duct seen in Fig. 4(*a*) shows how the rotational forces (dotted line) induce a migration of the cooler core flow toward the trailing surface in radially outward flow with the channel oriented at $\beta=90$ deg to the plane of rotation. This results in an increase of the heat transfer from the trailing surface, although it typically results in a decrease in heat transfer at the leading surface.

Tilting the smooth duct to $\beta=135$ deg causes the Coriolis forces to shift the secondary flow pattern from the case of $\beta=90$ deg. Now the secondary flow due to rotation travels along the line from the leading most corner of the duct to the trailing most corner of the duct. This results in a significant increase in heat transfer at the outer surface as well as a moderate increase for the entire leading and trailing surfaces. When ribs are installed as seen in Fig. 4(*b*), the combination of secondary flows produces a flow behavior that is entirely different from the smooth surface. The ribs induce a flow pattern parallel to the ribs at the wall, traveling from the upstream rib-half surface (from the outer surface in this case) to the downstream rib-half surface (toward the inner surface in this case). This rib configuration was chosen because when the channel is tilted to $\beta=135$ deg, the rib-induced secondary flow constructively combines with the rotation induced secondary flows. Past literature has paid little attention to the constructive and destructive combinations of rib and rotation-induced secondary flows. At $\beta=90$ deg, the rib-induced secondary flow constructively combines with the rotation-induced secondary flows at the leading-outer and trailing-inner surfaces, while the two secondary flows destructively combine at the trailing-outer and leading-inner surfaces. It is impossible to achieve completely constructive rib- and rotation-induced secondary flows in a channel of $\beta=90$ deg when using continuous ribs. If the ribs had been oriented with the upstream rib-half attached from the inner surface and the downstream rib-half following toward the outer surface, then a completely destructive combination of the rib and rotation-induced secondary flows would have resulted across the entire leading and trailing surfaces at the $\beta=135$ deg orientation. While it would be interesting to investigate such behavior, this analysis was limited to only the smooth and 45 deg rib orientation that produces constructive combinations of secondary flow.

Smooth Channel Results. Figures 5–7 contain the smooth duct data for three different channel configurations: stationary, rotation with $\beta=90$ deg and rotation with $\beta=135$ deg. Each case is subdivided into four experiments: (*a*) Re=5000, (*b*) Re=10000, (*c*) Re=20000, and (*d*) Re=40000. The corresponding rotation numbers for these cases are 0.305, 0.151, 0.075, and 0.038, respectively. Please reference Figure 1 for the data legend and surface locations within the channel. Figure 5 contains data for the stationary cases. The higher than asymptotic values in the normalized Nusselt number plots are attributable to the entrance effect in thermally developing flow. The plots all approach a horizontal asymptote as the flow approached the thermally fully developed state.

Figure 6 shows the results for the rotation cases where the duct is oriented at $\beta=90$ deg, that is, orthogonal to the plane of rotation. As was expected, the trailing surfaces exhibit higher heat transfer enhancement than the leading surfaces due to the migration of the colder core fluid toward the trailing surface caused by the Coriolis rotational forces. At a duct angle of $\beta=90$ deg, the channel can be assumed to hold symmetry about the plane of rotation. This means that both of the leading surfaces (leading-outer and leading-inner) should have identical Nu plots, the trailing surfaces should exhibit identical behavior, and the two side surfaces should be equal. This is validated relatively well as seen in the figures, with a slight bias between the two trailing surfaces. An increase in the Reynolds number tends to suppress the effect of rotation. All six surfaces show very little streamwise variation in the Nu number plots. Both of the side surfaces (inner and outer) have a heat transfer enhancement nearly equal to the value of the two trailing surfaces.

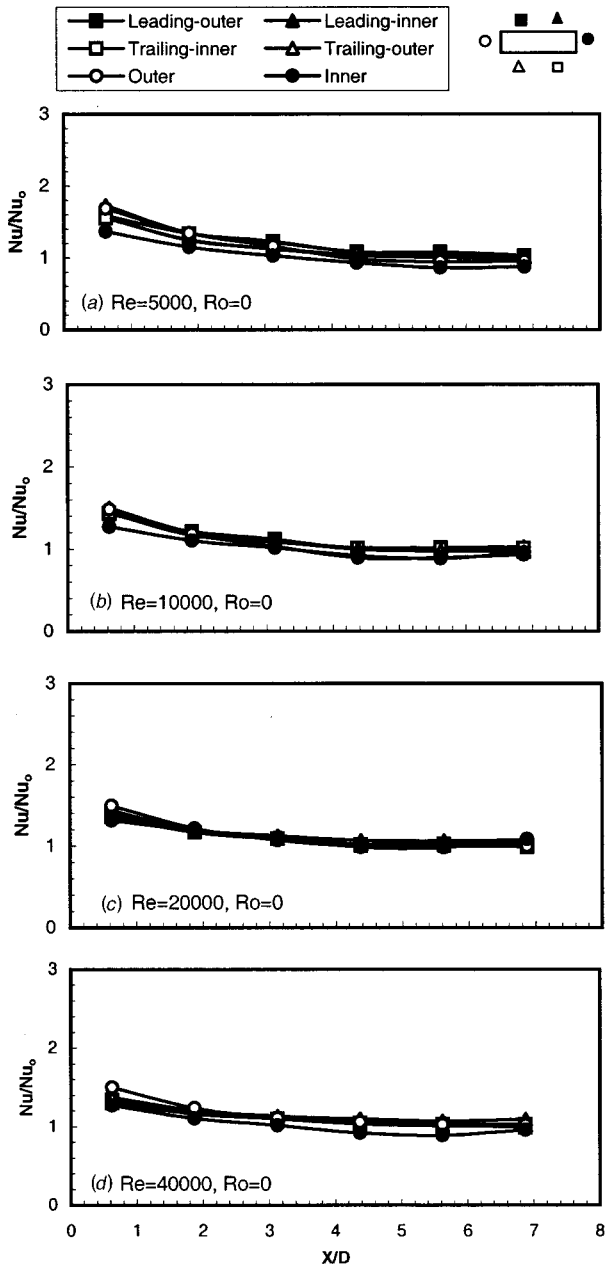

Fig. 5 Nusselt number ratio for stationary smooth case

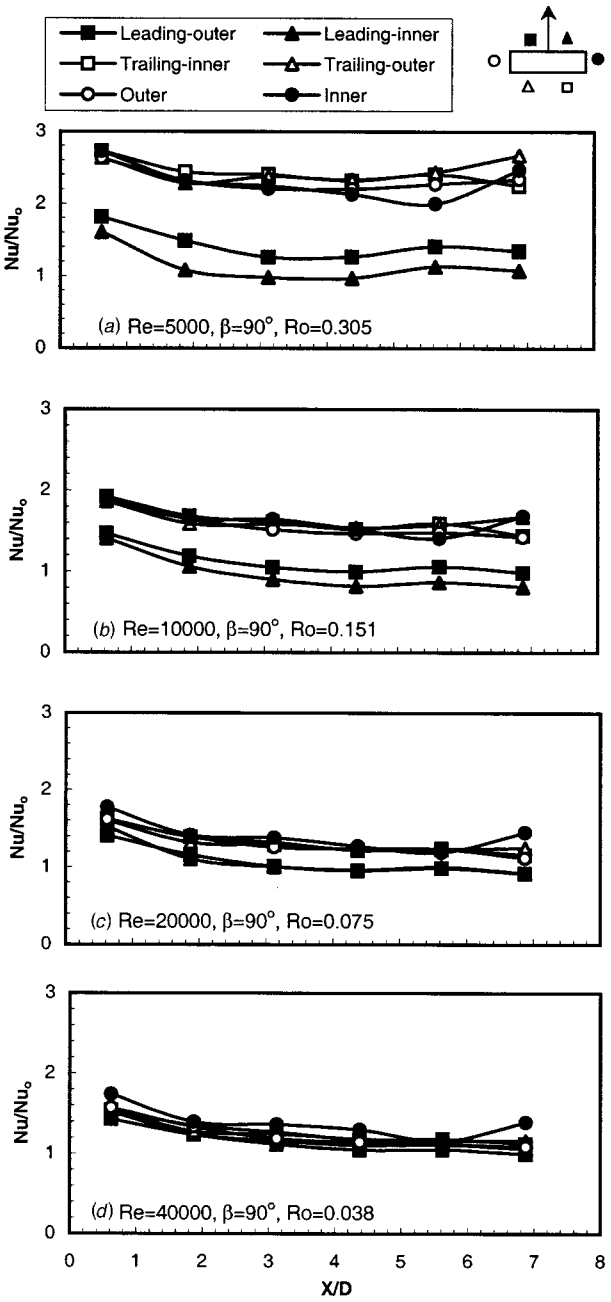

Fig. 6 Nusselt number ratio for rotation smooth case with $\beta=90$ deg

Figure 7 presents the results of the smooth rotation case with the channel oriented at $\beta=135$ deg with respect to the plane of rotation. Figure 7(a) shows that at a low Reynolds number (high rotation number), there are distinguishable differences in the heat transfer trends among the various surfaces. It can be seen that the trailing-outer and outer surface exhibit the highest heat transfer enhancement of all of the surfaces in the duct. This is attributed to the fact that these two surfaces are the primary recipients of the shifting of the cooler core flow under rotation. This phenomenon is illustrated in Fig. 4 of the preceding section. After the flow impinges on the trailing-outer and outer surfaces, it passes along the leading and trailing surfaces to the inner surface, where the heat transfer coefficient is the lowest, and the secondary flow slows down dramatically. Then the flow cycles again, passing from the leading most corner diagonally across the channel toward the trailing most corner. At a high rotation number, the inner surface heat transfer follows a trend quite similar to the stationary cases. It appears that this inner surface is barely affected by rotation. Both of the trailing surfaces have higher heat transfer coefficients than the leading surfaces. A new and interesting finding is the substantial difference in the heat transfer coefficient between the two trailing surfaces. Furthermore, this span-wise difference does not come into effect until nearly half-way through the channel for high rotation numbers (Ro=0.305). It is also shown that the leading surface heat transfer increased when compared to the orthogonal channel. The overall increase in heat transfer from nearly all surfaces can be attributed to the fact that twisting the channel greatly increased the linear distance along which the main Coriolis force is directed (from leading most to trailing most corner) and provides an overall better mixing than the $\beta=90$ deg. In the $\beta=90$ deg case, the principal Coriolis vector in the core region of the flow acts across only a short distance (the short width of the channel) and does not serve to mix the flow as well as the twisted channel.

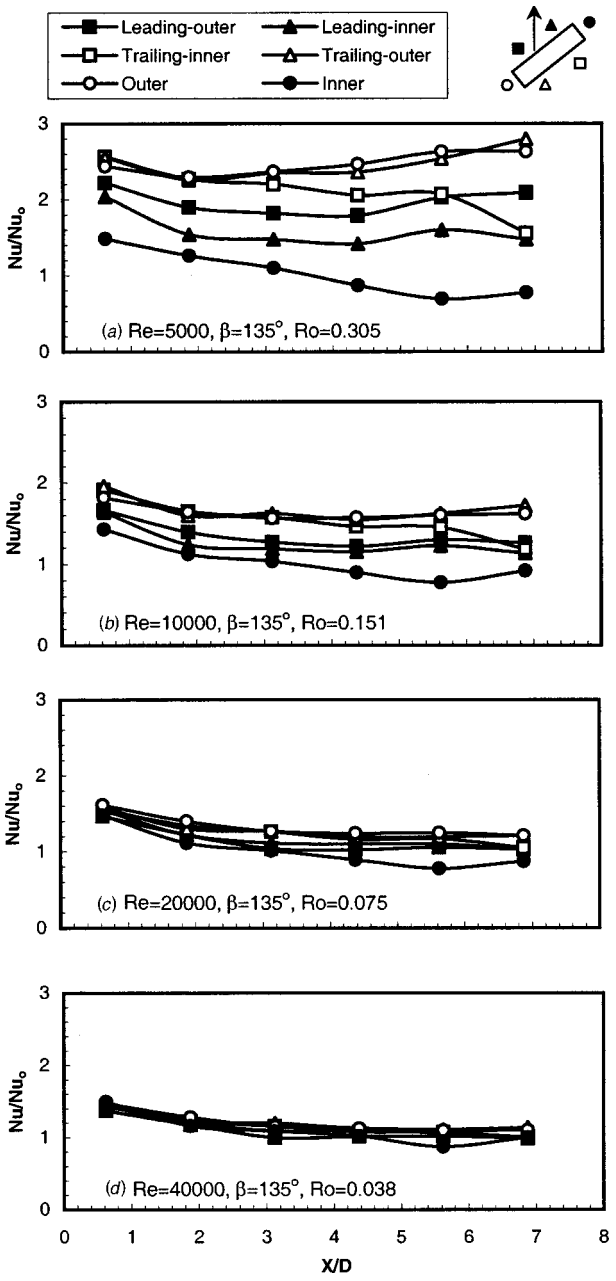

Fig. 7 Nusselt number ratio for rotation smooth case with $\beta = 135$ deg

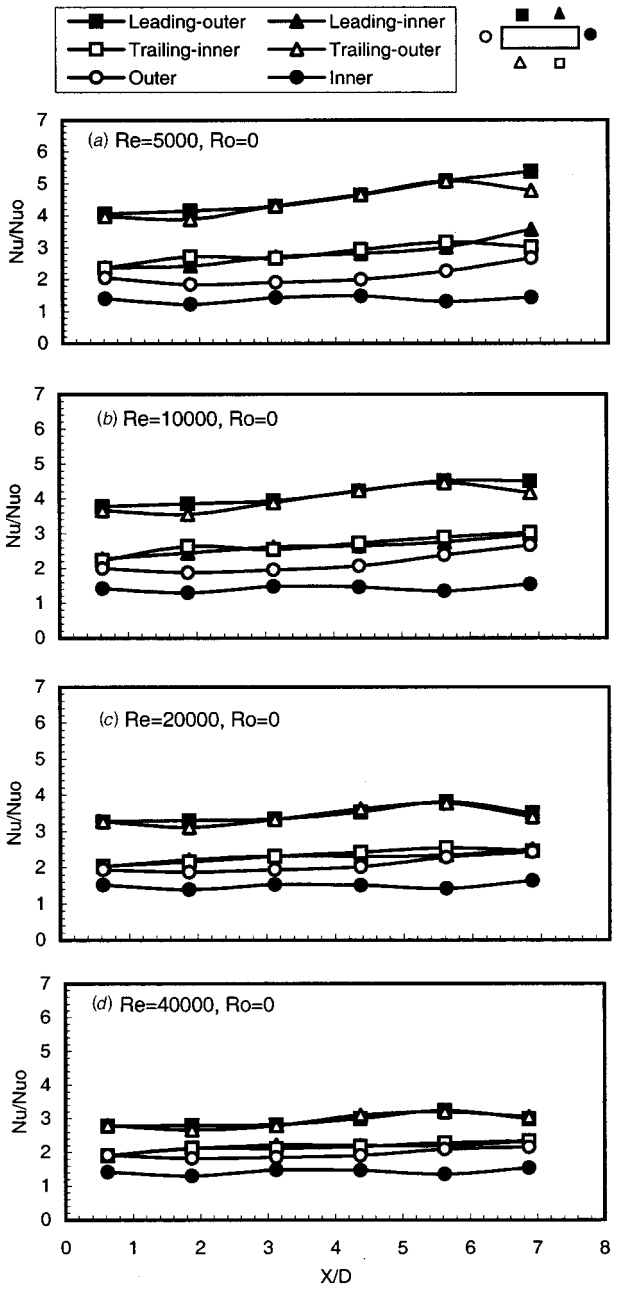

Fig. 8 Nusselt number ratio for stationary ribbed case

One evident contrast of the results of the $\beta = 135$ deg case (Fig. 7) compared to the $\beta = 90$ deg (Fig. 6) case is apparent in the side surfaces. For the twisted channel, the trend of the outer surface increases while the inner surface trend decreases with X/D. Furthermore, the inner surface decreases in a similar way as seen in the stationary case. The outer surface, which trails the inner surface, experiences a heat transfer enhancement of as much as three times that of the inner surface for the $\beta = 135$ deg case. This is due to the shift of the primary Coriolis induced flow vector from the center of the trailing surface in the $\beta = 90$ deg case to the trailing most corner in the $\beta = 135$ deg case. This trailing most corner is adjacent to the outer surface, and therefore the outer surface benefits greatly in heat transfer enhancement due to the twisting of the duct. This is desirable since the outer surface of the $\beta = 135$ deg case is closer to the trailing edge of the turbine blade, and thus is likely to experience a higher external heat flux than the inner surface. The inner surface interfaces with the side surface of the adjacent cooling passage, and therefore is less likely to be considered a critical surface.

Ribbed Channel Results. The data plots for the ribbed channel cases are presented in Figs. 8–10. Figure 8 shows the stationary ribbed channel data. It can be seen that the thermal entrance effect (decreasing to horizontal asymptote) that occurred in the smooth duct does not apply to the ribbed duct. This is due to the fact that the flow is no longer hydrodynamically fully developed immediately after the beginning of the test section, as was the case with the smooth duct. The ribs at the test section inlet trip the hydrodynamic boundary layer, and the flow is now considered not only thermally developing at the inlet, but also hydrodynamically developing at the inlet to the test section. In fact, the data curves tend to increase for the ribbed stationary case, whereas the plots decrease for the smooth stationary case.

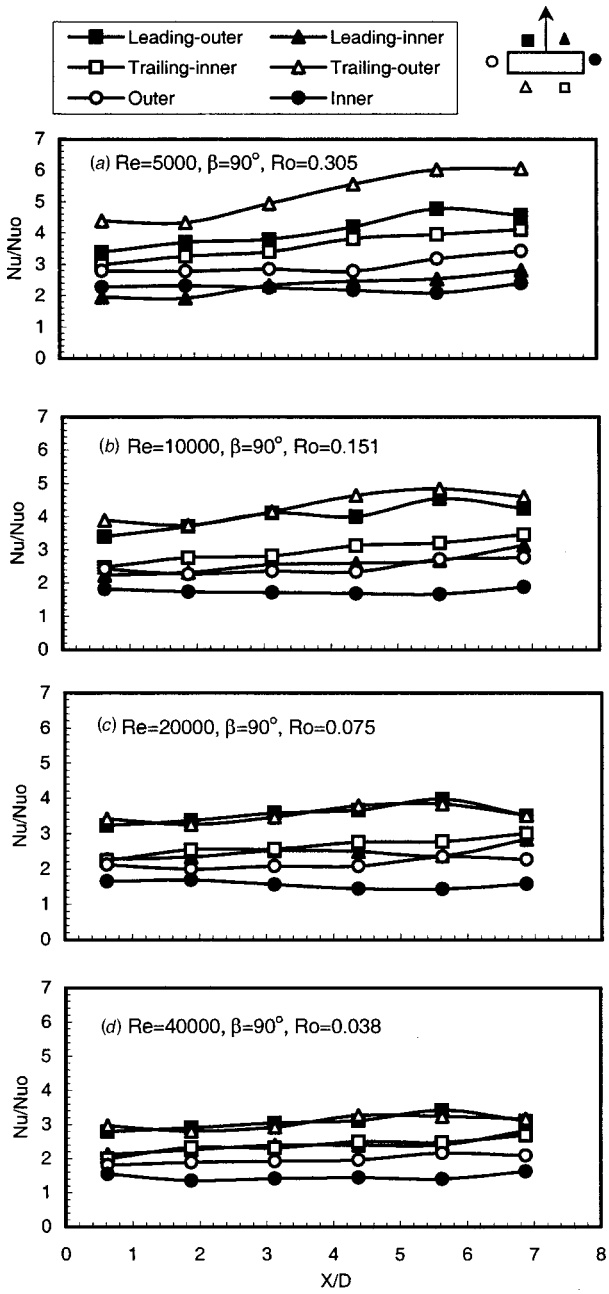

Fig. 9 Nusselt number ratio for rotation ribbed case with β=90 deg

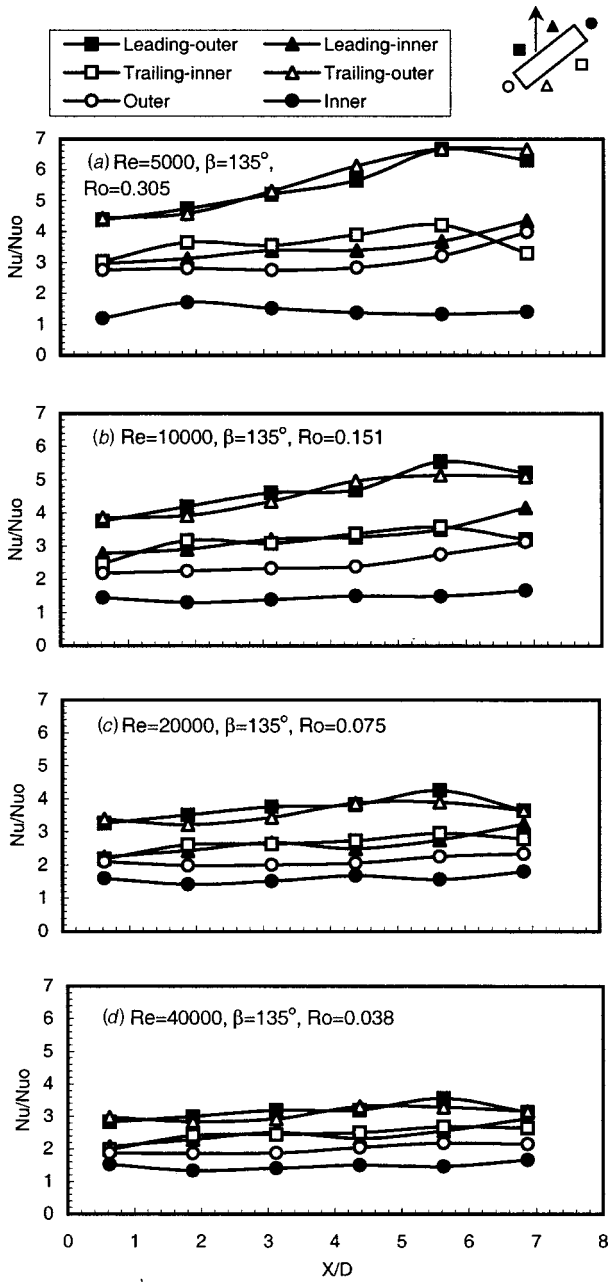

Fig. 10 Nusselt number ratio for rotation ribbed case with β=135 deg

An extremely important observation of this case is to note that the leading-outer and trailing-outer surfaces experience a significantly higher heat transfer enhancement than the leading-inner and trailing-inner surfaces. This is attributable to the orientation of the ribs. The ribs are attached such that the flow first meets the rib at the leading-outer and trailing-outer surfaces, which are the ''upstream rib-half'' surfaces (see Fig. 4). The second half of the rib, or ''downstream rib-half'' surface, follows as the rib extends toward the inner surface. Therefore, the ribs can be described as running from the outer surface to the inner surface at 45 deg to the main flow. As the flow first meets the rib at the upstream rib-half surface, the hydrodynamic boundary layer is tripped first at this point. The fluid at the ribbed wall is then channeled between the two ribs, flowing parallel to the ribs. The rib-induced secondary flow is fastest at the upstream rib-half surface, and slowing as it passes along the downstream rib-half surface toward the inner surface, which acts as a stagnation surface. The primary rib-half surface is able to convect more heat as the fluid passes quickly across the surface. When the flow slows along the downstream rib-half surface, less heat is convected away by the downstream rib-half surface. This explains why the leading-outer and trailing-outer (upstream rib-half) surfaces experience higher heat transfer than the leading-inner and trailing-inner (downstream rib-half) surfaces. Also, the outer surface has a higher heat transfer enhancement than the inner surface because it is peripherally affected by this faster, cooler, upstream rib-half tripped flow. In contrast, the inner surface experiences the heat transfer diminishing effects of flow stagnation.

The stationary rib cases show dependence on Reynolds number for the leading and trailing surfaces, however, the inner and outer surface exhibit nearly no dependence on Reynolds number. This is because as the Reynolds number increases, the rib is less effective

at enhancing the heat transfer of the rectangular duct when compared with the stationary smooth circular duct correlation (i.e., normalized Nu decreases). Since the ribs are attached to the leading and trailing surfaces, they experience much more of the enhancing effects of the ribs, and conversely, are affected more by a reduced enhancement of heat transfer at higher Reynolds numbers.

Figure 9 shows the data plots for the ribbed duct under rotation with an orientation orthogonal to the plane of rotation ($\beta = 90$ deg). Looking to Fig. 9(a), we can see that at higher rotation numbers, there is clearly a higher heat transfer from the trailing-outer surface, and an increasing trend with X/D. Also, the trend is similar to that of the stationary case. For this reason, the rib-induced flow is observed to dominate the rotation induced secondary flow. Another important observation is that the leading-inner surface exhibits nearly the lowest heat transfer enhancement at the highest rotation number.

Figure 10 presents the plots for the ribbed, $\beta = 135$ deg twisted channel rotation experiments. We immediately can see that by twisting the channel, the leading-outer surface curve rises to meet the trailing-outer surface curve, with the trailing-outer surface maintaining nearly the same trend as seen in the $\beta = 90$ deg case. Even the trailing-outer surface trend increases slightly over that of the $\beta = 90$ deg case. From this behavior, it seems as though the effects of rotation for the twisted channel serve to better mix the flow than the orthogonal channel, and most of the surfaces benefit from the entirely constructive combining of rib and rotation-induced secondary flows for the $\beta = 135$ deg case. That is, all surfaces benefit except the inner surface, which is the only surface in the twisted channel to exhibit a lower heat transfer when compared with the orthogonal channel. This is expected because the heat transfer at the inner surface is now mitigated by not only its position as the leading most surface, but also by being situated at the end of the downstream rib-half. Since the inner surface is likely to be the surface exposed to the side wall of an adjacent cooling passage, a low heat transfer is not foreseen to be a significant problem. Therefore, we can say that the attachment scheme for continuous ribs chosen in this investigation will likely provide the most effective heat transfer augmentation at the necessary surfaces.

Streamwise Averaged Nusselt Number Ratio. An overall heat transfer coefficient for each surface is determined by averaging the streamwise data and then plotting the data as a function of rotation number. Figure 11 shows the streamwise averaged data for the smooth duct. Figure 11(a) ($\beta = 90$ deg) shows that the heat transfer at the trailing surfaces, the inner surface and the outer surface, is a strong function of rotation number. All four of these surfaces exhibit an increasing trend with increasing rotation number. The two leading surfaces show very little dependence on rotation number. Figure 11(b) ($\beta = 135$ deg) shows that the trailing surfaces are strongly dependent on rotation number. The inner surface is the only surface that shows virtually no dependence on rotation number for this case. A comparison of Figs. 11(a) and 11(b) reveals that the two leading surfaces for the $\beta = 135$ deg case are more dependent on rotation number than for the $\beta = 90$ deg case. These results are different than the results of the square channel of Dutta and Han [7] and the 2:1 rectangular channel investigated by Azad et al. [16]. A comparison of the 4:1 duct with the square and the 2:1 duct reveals that the aspect ratio significantly affects the rotational dependence on heat transfer, particularly for the leading surface. The square duct shows a decreasing trend, the 2:1 duct approaches a nearly horizontal trend, while the 4:1 duct shows an increasing trend. Therefore, as the channel becomes narrower, the heat transfer enhancement at the leading surfaces becomes more positive. It is now conclusive that the aspect ratio significantly affects the heat transfer distribution in the channel.

Figure 12 shows the streamwise averaged heat transfer enhancement for the ribbed duct. For the orthogonal channel of Fig.

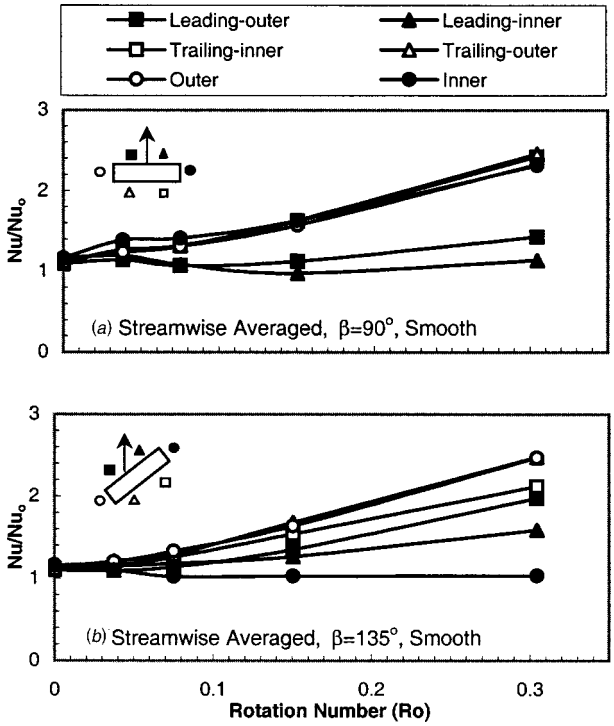

Fig. 11 Streamwise averaged Nusselt number ratio for smooth channel

12(a), the trailing surfaces and outer surface show an increasing trend with increasing rotation number. The trailing-outer surface exhibits the greatest dependence on rotation number, which is a result of the combination of rib and rotation-induced heat transfer enhancement. The leading surfaces exhibit little dependence on rotation number. Figure 12(b) shows that all surfaces are a function of rotation number except the inner surface. Furthermore, the twisted channel produces a nearly identical trend for the two up-

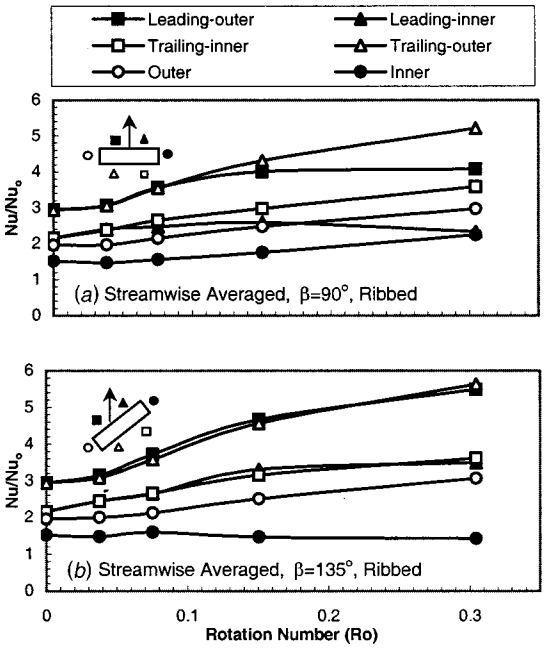

Fig. 12 Streamwise averaged Nusselt number ratio for ribbed channel

stream rib-half surfaces (leading-outer and trailing-outer). Also, the downstream rib-half surfaces (leading-inner and trailing-inner) show very similar trends. A comparison of Figs. 12(*a*) and 12(*b*) shows that the leading surfaces and the inner surface are positively affected by the channel orientation. The trailing surfaces and the outer surface appear to be unaffected by the channel orientation.

Conclusions

This investigation revealed that spanwise heat transfer differences of up to 25 percent for the smooth tilted channel and 50–75 percent for the ribbed channel exist across the leading and trailing surfaces. This observation should be addressed when designing the cooling channels of a gas turbine blade. In addition, the duct orientation significantly affects the leading, the inner, and the outer surfaces, yet does not have much effect on the trailing surfaces for both the smooth and ribbed cases. Furthermore, the smooth and ribbed case trailing surfaces and the smooth case side surfaces show a strong dependence on rotation number. Finally, the aspect ratio was determined to affect the leading surface heat transfer enhancement, where the enhancement increases as the channel becomes narrower. Therefore, this investigation has determined that spanwise variations in the heat transfer distribution of rectangular cooling passages exist and that the enhancement is a function of channel orientation, surface configuration, and aspect ratio.

Acknowledgments

The Advanced Gas Turbine Systems Research (AGTSR) program (project number SR-082) funded this experimental investigation under the supervision of the United States Department of Energy (DOE). The authors greatly appreciate the support of the AGTSR program and the DOE. Without such support, this research would not have been possible.

Nomenclature

A_p = surface area of copper plate (m^2)
D = hydraulic diameter (m)
e = rib height (m)
h = heat transfer coefficient (W/m^2 K)
k = thermal conductivity of coolant (W/mK)
L = length of duct (m)
Nu = regionally averaged Nusselt number, hD/k
Nu_o = Nusselt number in fully developed turbulent nonrotating tube flow without ribs
P = rib pitch (m)
Pr = Prandtl number
Q = heat transfer (W)
q''_{net} = net heat flux at wall (W/m^2)
R = mean rotating radius (m)
Re = Reynolds number, $\rho VD/\mu$
R_o = rotation number, $\Omega D/V$
T_{bx} = local coolant bulk temperature (K)
T_w = wall temperature (K)
V = bulk velocity in streamwise direction (m/s)
β = angle of channel orientation
Ω = rotational speed (rad/s)
α = rib angle
ρ = density of coolant (kg/m^3)
$(\Delta\rho/\rho)_i$ = coolant-to-wall density ratio at the inlet, $(\rho_w-\rho_{bi})/\rho_w=(T_w-T_{bi})/T_w$

References

[1] Han, J. C., and Park, J. S., 1988, "Developing Heat Transfer in Rectangular Channel With Rib Turbulators," Int. J. Heat Mass Transf., **31**(1), pp. 183–195.
[2] Han, J. C., Zhang, Y. M., and Lee, C. P., 1991, "Augmented Heat Transfer in Square Channels With Parallel, Crossed, and V-Shaped Angled Ribs," ASME J. Heat Transfer, **113**, pp. 590–596.
[3] Wagner, J. H., Johnson, B. V., and Hajek, T. J., 1991, "Heat Transfer in Rotating Passage With Smooth Walls and Radial Outward Flow," ASME J. Turbomach., **113**, pp. 42–51.
[4] Wagner, J. H., Johnson, B. V., and Kooper, F. C., 1991, "Heat Transfer in Rotating Serpentine Passage With Smooth Walls," ASME J. Turbomach., **113**(3), pp. 321–330.
[5] Parsons, J. A., Han, J. C., and Zhang, Y. M., 1995, "Effects of Model Orientation and Wall Heating Condition on Local Heat Transfer in a Rotating Two-Pass Square Channel With Rib Turbulators," Int. J. Heat Mass Transf., **38**(7), pp. 1151–1159.
[6] Johnson, B. V., Wagner, J. H., Steuber, G. D., and Yeh, F. C., 1994, "Heat Transfer in Rotating Serpentine Passage With Selected Model Orientations for Smooth or Skewed Trip Walls," ASME J. Turbomach., **116**, pp. 738–744.
[7] Dutta, S., and Han, J. C., 1996, "Local Heat Transfer in Rotating Smooth and Ribbed Two-Pass Square Channels with Three Channel Orientations," ASME J. Heat Transfer, **118**, pp. 578–584.
[8] Al-Qahtani, M., Jang, Y., Chen, H. C., and Han, J. C., 2001, "Prediction of Flow and Heat Transfer in Rotating Two-Pass Rectangular Channels with 45 deg Rib Turbulators," ASME Paper No. 2001-GT-0187.
[9] Taslim, M. E., Rahman, A., and Spring, S. D., 1991, "An Experimental Investigation of Heat Transfer Coefficients in a Spanwise Rotating Channel With Two Opposite Rib-Roughened Walls," ASME J. Turbomach., **113**, pp. 75–82.
[10] Taslim, M. E., Bondi, L. A., and Kercher, D. M., 1991, "An Experimental Investigation of Heat Transfer in an Orthogonally Rotating Channel Roughened With 45 deg Criss-Cross Ribs on Two Opposite Walls," ASME J. Turbomach., **113**, pp. 346–353.
[11] Willett, F. T., and Bergles, A. E., 2000, "Heat Transfer in Rotating Narrow Rectangular Ducts with Heated Sides Oriented at 60 deg to the R-Z Plane," ASME Paper No. 2000-GT-224.
[12] Han, J. C., Dutta, S., and Ekkad, S. V., 2000, *Gas Turbine Heat Transfer and Cooling Technology*, Taylor and Francis, New York.
[13] Han, J. C., and Dutta, S., 2001, "Recent Developments in Turbine Blade Internal Cooling," in *Heat Transfer in Gas Turbine Systems*, R. J. Goldstein, ed., Ann. N.Y. Acad. Sci., **934**, pp. 162–178.
[14] Dutta, S., and Han, J. C., 1998, "Rotational Effects on the Turbine Blade Coolant Passage Heat Transfer," Annu. Rev. Heat Transfer, **9**, pp. 268–314.
[15] Kline, S. J., and McClintock, F. A., 1953, "Describing Uncertainties in Single-Sample Experiments," Mech. Eng. (Am. Soc. Mech. Eng.), **75**, pp. 3–8.
[16] Azad, G. S., Uddin, J. M., Han, J. C., Moon, H. K., and Glezer, B., 2001, "Heat Transfer in a Two-Pass Rectangular Rotating Channel with 45 deg Angled Rib Turbulators," ASME Paper No. 2001-GT-0186.